Journal of Applied Electrochemistry (2006) 36:11–16
DOI 10.1007/s10800-005-9016-8

Enhanced electrochemical properties of nonstoichiometric amorphous $Mg_2Ni_{1.3}$ electrodes

Z. P. GUO*, Z. G. HUANG, Z. W. ZHAO, X. MENARD and H. K. LIU
Institute for Superconducting and Electronic Materials, University of Wollongong, NSW, 2522, Australia
*(*author for correspondence, fax: +61-2-4221-5731, e-mail: zguo@uow.edu.au)*

Received 17 January 2005; accepted in revised form 9 May 2005

Key words: electrochemical properties, $Mg_2Ni_{1.3}$, nonstoichiometric

Abstract

Nonstoichiometric amorphous $Mg_2Ni_{1.3}$ alloys were synthesized by mechanically milling crystalline Mg_2Ni alloy with Ni powders. In comparison with the stoichiometric material, the nonstoichiometric $Mg_2Ni_{1.3}$ phase showed a higher discharge capacity because of the amorphization of the alloy. Surface modification with graphite was also carried out for further improvement of its electrode performance. The coated powders showed a better cyclic stability because the graphite protected the Mg from oxidation. The rate capability (RC) and discharge capacity of electrodes was also markedly improved with graphite coating due to the excellent electrical conductivity and electrocatalytic activity of graphite.

1. Introduction

Mg-based nanocrystalline/amorphous alloys have attracted great attention as negative electrodes in metal hydride batteries and potential hydrogen storage materials for fuel cell vehicles due to their high hydrogen storage capacities [1]. However, the reaction of Mg_2Ni alloys with hydrogen requires quite high temperatures (200–300 °C) and pressures (up to 10 atm) due to hydriding/dehydriding difficulties [2]. The kinetics of hydriding and dehydriding are slow. It is almost impossible to absorb and desorb hydrogen in Mg_2Ni at either one atmosphere or room temperature in a gaseous environment. Thus an electrochemical approach was used in our laboratory to investigate the hydriding/dehydriding characteristics of Mg_2Ni-based alloys. In recent years, it has been shown that the most effective way for Mg-based hydrogen storage alloy electrodes to achieve high discharge capacities is by mechanical alloying [3, 4] and mechanical milling (MM) of the Mg-based hydrogen storage alloys with Ni powders [5, 6]. After mechanical milling, the most important change in the Mg-based alloys is that they have completely or mainly amorphous structures. It is believed that the diffusivity and solubility of hydrogen in amorphous metal hydrides are larger than those in the crystalline phase, since amorphous alloys do not have a long range order but only nearest neighbor or local order [7, 8].

In our previous work [9], nonstoichiometric amorphous Mg-based alloy with a discharge capacity of 400 mAh g^{-1} was successfully synthesized by mechanical milling. But the cyclic stability of the nonstoichiometric amorphous Mg-based alloys is very poor so that only about 20% of the maximum capacity remains after 10 cycles. Although the application of a mechanical milling process for producing Mg-based alloy looks promising, oxidation on the alloy surface was also a serious problem, leading to low discharge capacity, poor cycle performance, etc.

In this work, nonstoichiometric amorphous Mg-based alloys were synthesized by mechanically milling crystalline Mg_2Ni alloy with Ni powders. It has been found that the microstructure and electrochemical properties of ball-milled $Mg_2Ni_{1+x}(0 < x < 1)$ composites depend greatly on the amount of Ni introduced during ball-milling. Under the ball-milling conditions we used, as the x value is increased from 0.1 to 0.3, the alloy particles become smaller and smaller. A large fresh surface is generated, and hence the opportunities for surface electrochemical reactions and charge transfer increase. However, with further increases in x, small particles start to agglomerate due to exceeding the optimum grinding time, thus leading to the deterioration of electrocatalytic activity and the charge transfer reaction. Therefore, we chose to study the optimum composition $Mg_2Ni_{1.3}$ alloy. Although much work has been done on Mg-based alloy, to our knowledge there are no investigations on the $Mg_2Ni_{1.3}$ system. The $Mg_2Ni_{1.3}$ alloy has an amorphous structure, resulting in high discharge capacities in comparison with crystalline Mg_2Ni alloy. Surface modification (mechanical coating) with graphite elemental powders was conducted in order to further improve the electrode performance of Mg-based alloys.

2. Experimental

2.1. *Alloy preparation and characterization*

The polycrystalline Mg_2Ni alloy was prepared from Mg and Ni mixed powders by sintering at 700 °C in argon for 10 h. Mechanical milling was performed with a Fritsch (P5) planetary ball mill to obtain nanocrystalline/amorphous Mg-based alloy. The vial and balls were made from stainless steel and hardened steel, respectively. To obtain more active alloy powders, the Mg_2Ni alloy was mixed and ball milled with Ni powder for 70 h at 200 rpm in an argon atmosphere. To prolong cycle life, further mechanical coatings with graphite were carried out. A two-step milling process was introduced for the coating process. In the first step, only graphite powder was charged and milled for 30 min at 200 rpm with a ball to powder ratio of 30:1 to make it suitable for coating. Then, the pre-milled coating powders and milled alloy powders were ball milled at 100 rpm for 2 h with a ball to powder ratio of 20:1. After milling, the powders were examined by XRD using a Philips 1730 x-ray diffractometer with CuKα radiation. Morphologies of the powdered alloys were studied with a Leica Stereoscan 440 scanning electron microscope (SEM).

2.2. *Electrochemical measurements*

The Mg-based alloys obtained were mixed with Ni powder in the weight ratio of 1:1 to make electrodes. The hydride electrodes were fabricated by mixing the resultant powders with polyvinyl alcohol (PVA) solution and pasting them into a foamed nickel matrix, which acted as the current collector for the electrode. After being compressed, the hydride electrodes were immersed as negative electrodes in a 6 M KOH solution together with a $NiOOH/Ni(OH)_2$ positive electrode. The electrochemical charge–discharge properties of the alloys were measured using a battery test unit controlled by a computer at room temperature. In the charge–discharge cycle tests, the charge cycle was commenced using a current density of 100 mA g^{-1} of hydrogen storage alloy for 10 h. Then, after 10 min rest, the discharge was continued using a current density of 50 mA g^{-1} until the voltage of the cell reached 0.9 V.

3. Results and discussion

3.1. *Structural properties*

The XRD pattern of the sintered Mg_2Ni is shown in Figure 1(a), which indicates a mainly Mg_2Ni phase with a small amount of MgO present as an impurity. Figure 1(b) shows the XRD pattern of the sintered Mg_2Ni alloy that was ball milled for 70 h. A nanocrystalline Mg_2Ni phase with broadened diffraction peaks was observed. The peak broadening means a decreased average crystallite size and an increase in the internal strain due to mechanical deformation during ball milling [10]. Two small peaks were identified as metallic Ni. Figure 1(c) shows the XRD pattern of the sintered Mg_2Ni alloy ball-milled with Ni powders in a molar ratio of 1:0.3, indicating that homogenous amorphous $Mg_2Ni_{1.3}$ alloy was formed. By comparing Figure1(b) and (c), it may be noted that amorphisation of the alloy could be easier with further addition of Ni powder. Similar observations on amorphous phase formation have been reported elsewhere [11, 12]. Figure 2 shows an SEM micrograph of the 70 h ball milled $Mg_2Ni_{1.3}$ powders. The sample consists of welded particles with a size of several micrometers. The powder surface of $Mg_2Ni_{1.3}$ alloy looks defective, implying that it should be a more activated amorphous surface with

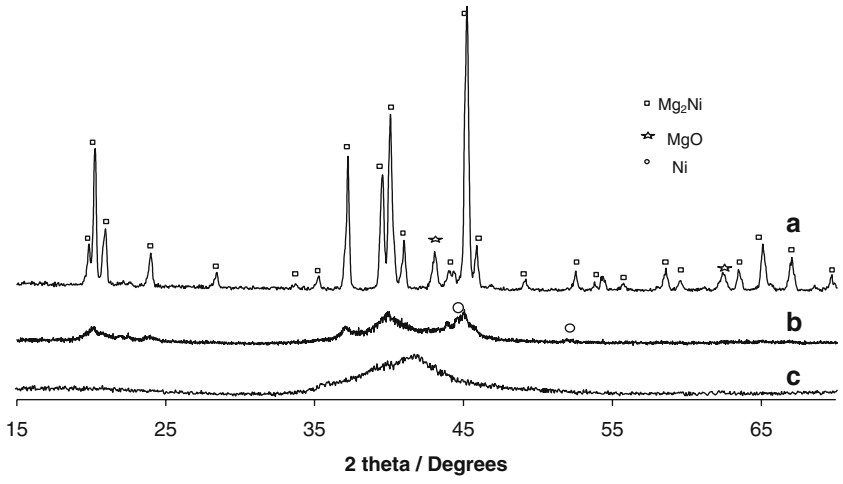

Fig. 1. XRD patterns of the Mg-based alloys (a) sintered Mg_2Ni; (b) Mg_2Ni after milling for 70 h; (c) $Mg_2Ni_{1.3}$ after milling for 70 h.

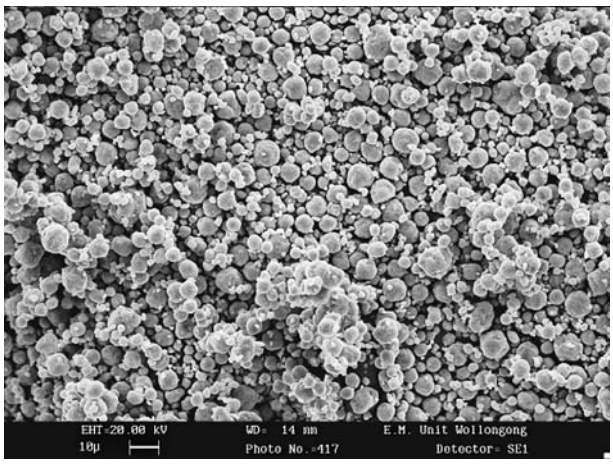

Fig. 2. SEM micrograph of the $Mg_2Ni_{1.3}$ alloy powders without graphite coating.

high catalytic activity [9]. Since Mg is very susceptible to oxidation, EDX mapping of the different elements was conducted to analyse the distribution of the species within the welded particles (Figure 3). The bright spots indicate the presence of each particular element. Based on the EDX elemental maps, Mg and Ni in the $Mg_2Ni_{1.3}$ sample after milling for 70 h are completely well-distributed, while there is small amount of oxygen (7.5 atom%). The oxygen may come from two sources, i.e. the sintered Mg_2Ni (since MgO peaks were found in the XRD pattern of sintered Mg_2Ni) and absorbed air. The molar ratio between Mg and Ni is 1:0.653, very close to the theoretical ratio, indicating that the Mg volatilization during preparation is acceptable.

3.2. *Electrochemical properties*

The decrease in the discharge capacities of the nanocrystalline Mg_2Ni, amorphous $Mg_2Ni_{1.3}$ and $Mg_2Ni_{1.3}$ coated with graphite, after repeated charge/discharge cycles at a discharge current density of 50 mA g^{-1} is shown in Figure 4. The discharge capacities of the alloys were calculated using their total weights. The maximum discharge capacity was observed at the 1st cycle in all cases. The nanocrystalline Mg_2Ni alloy has a relatively low discharge capacity, while amorphous alloys of $Mg_2Ni_{1.3}$ with or without graphite coating have much higher capacities, 395 mAh g^{-1} and 450 mAh g^{-1}, respectively. Capacity fading was observed after several charge/discharge cycles in all alloys, but the decay of the discharge capacity for $Mg_2Ni_{1.3}$ with or without graphite coating was far slower compared to the Mg_2Ni negative electrode. Discharge curves at the 1st cycle of the Mg-based negative electrodes are shown in Figure 5. The plateau potential for the $Mg_2Ni_{1.3}$ electrode is higher than that of Mg_2Ni. $Mg_2Ni_{1.3}$ coated with graphite shows the highest plateau potential. These results suggest that the increase in the equilibrium hydrogen pressure and improvement in the electrochemical reactivity on the alloy surface leads to improved dischargeability [13].

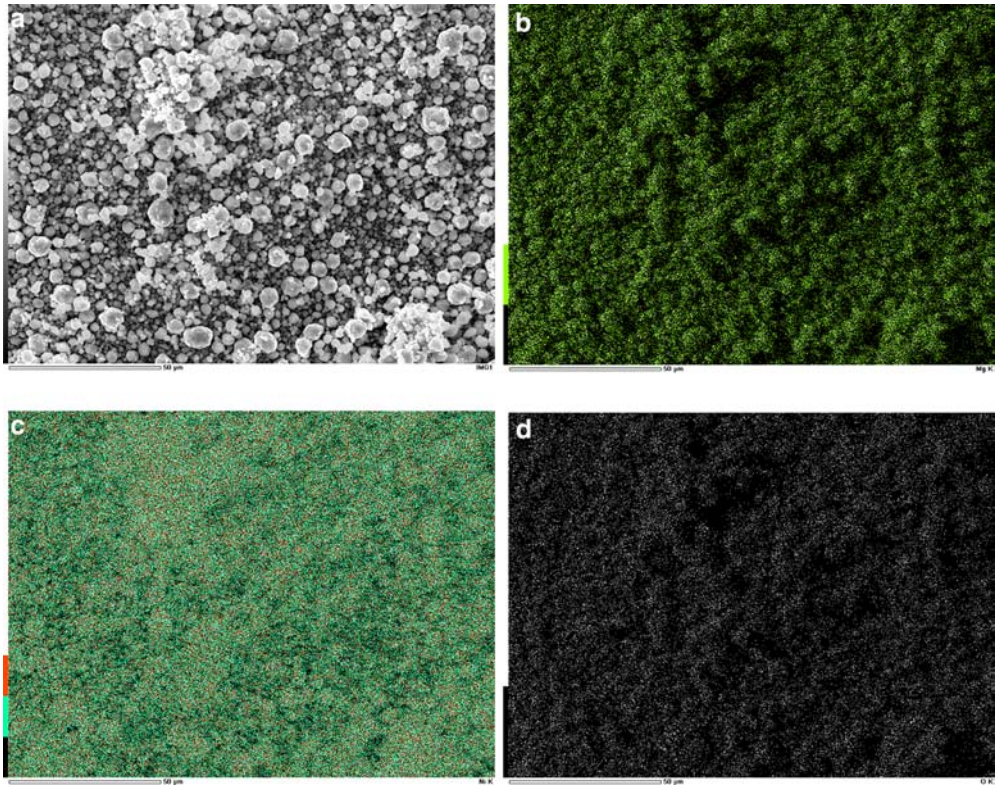

Fig. 3. SEM and chemical map of (b) Mg, (c) Ni and (d) O for the $Mg_2Ni_{1.3}$ alloy obtained after milling for 70 h.

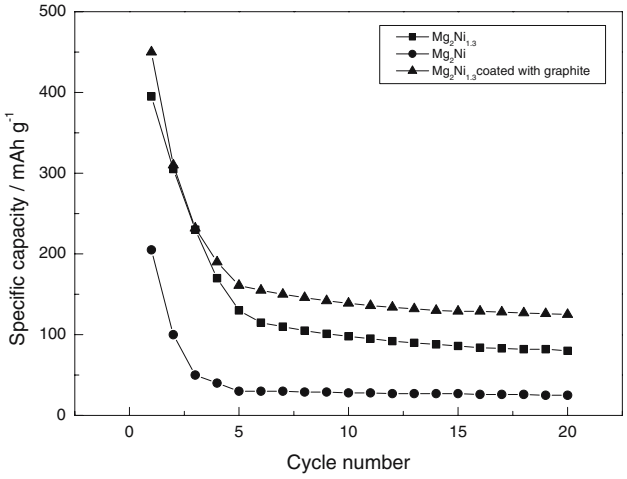

Fig. 4. Discharge capacities of the Mg-based alloys after repeated charge/discharge cycles at a discharge current density of 50 mA g^{-1}.

It has been well known since the 1960s that amorphous metals and alloys can be made by rapid quenching from the vapor or the liquid phase. A large number of investigation have shown that amorphous metals and alloys have the features of new alloy compositions along with new atomic configurations which are totally different from those of crystalline alloys. These features enable various kinds of characteristics to be achieved, such as excellent mechanical properties, useful physical properties and unique chemical properties [14–16]. The hydriding reaction mechanism of the amorphous phase is not clear, and there are some conflicting reports on the hydriding/dehydriding properties of amorphous hydride. However, it is believed that the diffusivity and solubility of hydrogen in amorphous metal hydride are larger than those in the crystalline phase [7, 8]. Therefore, it seems likely that the large discharge capacities of amorphous $Mg_2Ni_{1.3}$ are related to the amorphization and the decrease in binding energy of Mg at the surface.

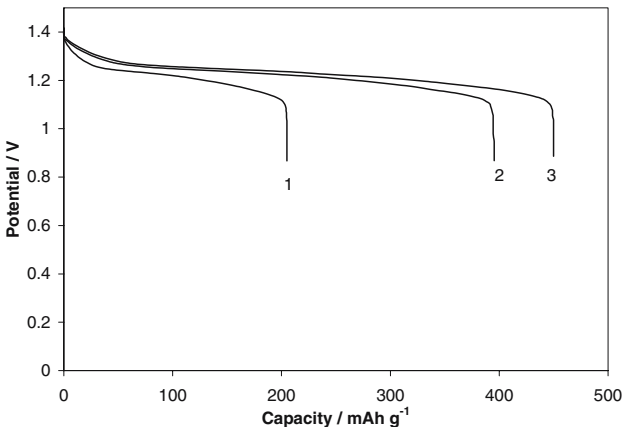

Fig. 5. Discharge curves at 1st cycle of the Mg-based electrodes. Discharge current density: 50 mA g^{-1}. (1) nanocrystalline Mg_2Ni alloy; (2) amorphous $Mg_2Ni_{1.3}$ alloy; (3) $Mg_2Ni_{1.3}$ coated with graphite.

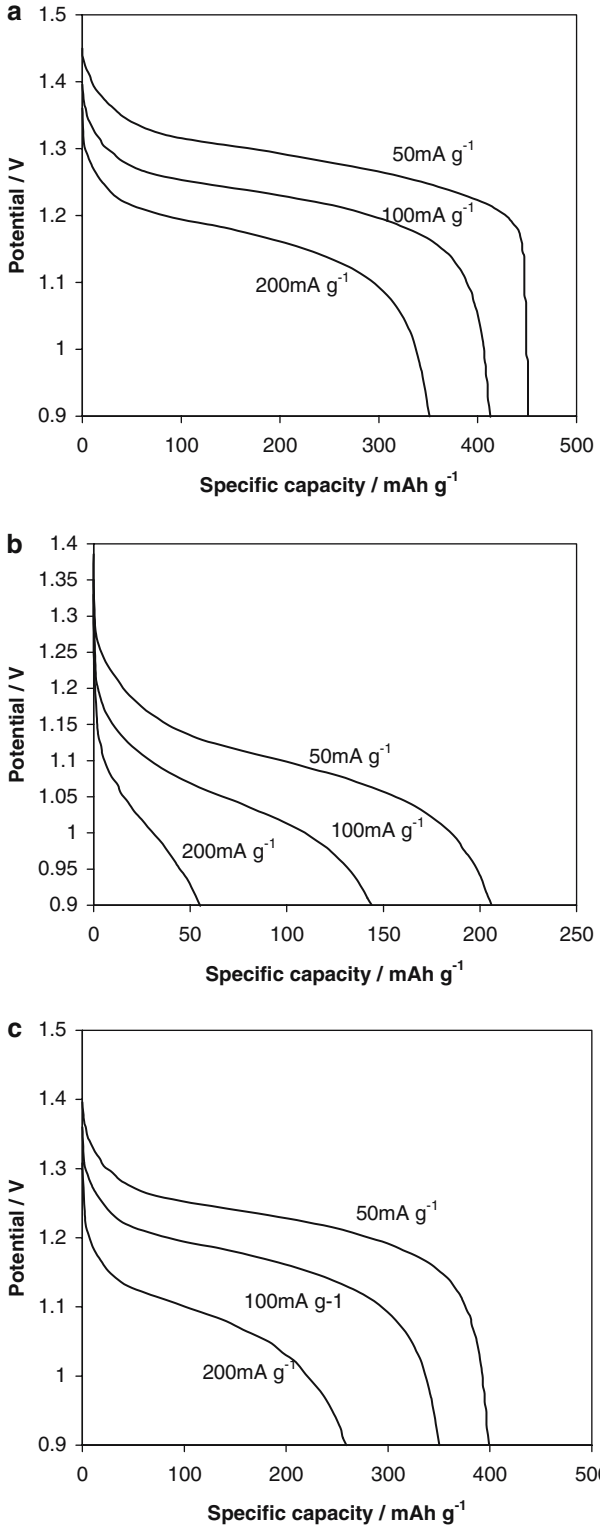

Fig. 6. Discharge curves (1st cycle) of the Mg-based alloy negative electrodes at different discharge current densities. (a) $Mg_2Ni_{1.3}$ coated with graphite; (b) nanocrystalline Mg_2Ni alloy; (c) amorphous $Mg_2Ni_{1.3}$ alloy.

Graphite coating using the mechanical coating method has been used in this study because it does not require an addition process or the use of a toxic solution as in the case of chemical coating. The electrodes prepared from the coated powders had

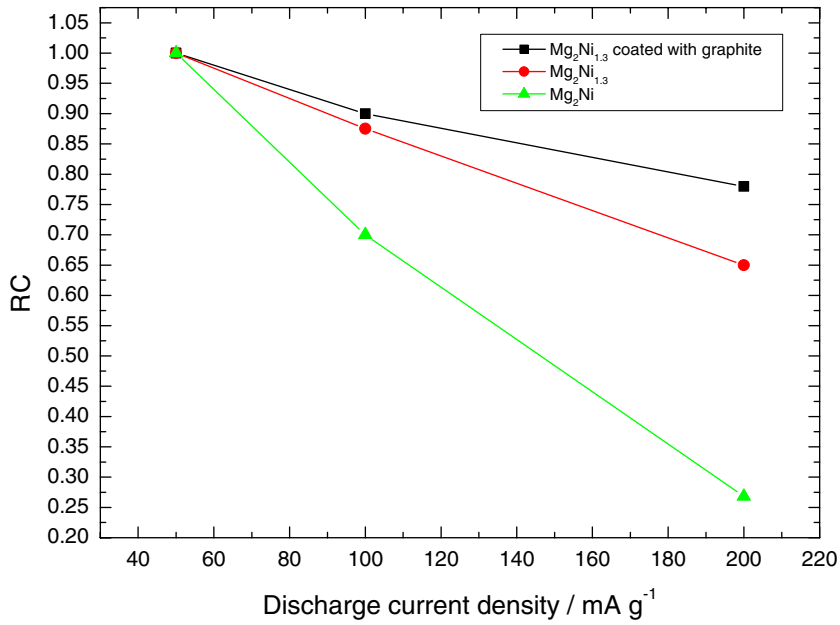

Fig. 7. RC values as a function of discharge current density for the Mg-based alloy negative electrodes.

higher electrode capacity because of the excellent electrical conductivity and electrocatalytic activity of graphite. The cyclic stability was also slightly improved compared with the bare ones because the graphite coating protected the Mg from oxidation [17].

Besides discharge capacity and cycle performance, rate capability is another important factor for batteries. However, there have been few reports on the rate capability of Mg_2Ni-based alloy negative electrodes to our knowledge. In this study, the rate capability of Mg_2Ni-based alloy with and without graphite coating was also investigated. Figure 6 shows discharge curves (1st cycle) of Mg-based negative electrodes at different discharge current densities. The discharge capacity decreased with increasing discharge current density in all cases, and the Mg_2Ni electrode shows the largest decrease in the discharge capacity (Figure 6(b)). The smallest decrease in the discharge capacity was observed in the $Mg_2Ni_{1.3}$ coated with graphite electrode (Figure 6(a)). For all electrodes, the rate capability (RC) value was plotted as a function of the discharge current density, and the results are shown in Figure 7. The RC is defined as follows

$$RC(\%) = (C_i/C_{50}) \times 100$$

where C_i and C_{50} are discharge capacities at a given discharge current density (i mA g^{-1}) and 50 mA g^{-1}, respectively. The increase in discharge current density decreased the RC value and its decrease was smaller for the $Mg_2Ni_{1.3}$ sample. In particular, a high RC value (78%) was obtained for the $Mg_2Ni_{1.3}$ coated with graphite. It was reported that the hydrogen in the amorphous phase of the alloy was destabilized, leading to accelerated hydrogen diffusion [13]. This is likely to be a factor for the improvement in rate capability in amorphous $Mg_2Ni_{1.3}$ electrodes. For the $Mg_2Ni_{1.3}$ coated with graphite, rate capability was further improved because the graphite coating improves the electrical contact between particles; therefore, the polarization of the electrode during charging/discharging decreased.

In summary, nonstoichiometric amorphous $Mg_2Ni_{1.3}$ alloy can be achieved by the mechanical milling method. The nonstoichiometric $Mg_2Ni_{1.3}$ electrode showed better electrochemical performance than stoichiometric Mg_2Ni alloy in terms of initial discharge capacity, cyclic stability and rate capability, because of the formation of an amorphous phase induced by Ni addition. Graphite coating can further improve the capacity and rate capability.

Acknowledgements

The authors thank Dr. K. Konstantinov for his help in the SEM measurements. Financial support from the Australia Research Council through Grants No. DP0449660, is gratefully acknowledged.

References

1. J.C. Bolcich, A.A. Yawuy, H.L. Corso, H.A. Pertti and C.O. Anala, *Int. Hydrogen Energy* **19** (1994) 605.
2. Q.D. Wang in Proceedings of the Second Pacific Rim International Conference on Advanced Materials and Processing, 1995 (Korea: The Korea Institute of Metal and Materials) 1529.
3. W.H. Liu, H.Q. Wu, Y.Q. Lei, Q.D. Wang and J. Wu, *J. Alloys Compd.* **261** (1997) 289.
4. S. Nohara, K. Hamasaki, S.G. Zhang, H. Inoue and C. Iwakura, *J. Alloys Compd.* **280** (1998) 104.

5. L. Sun, H.K. Liu, D.H. Bradhurst and S.X. Dou, *Electrochem. Solid-State Lett*. **2** (1999) 164.
6. L. Sun, Y. Pei, H.K. Liu, D.H. Bradhurst and S.X. Dou, *J. Alloys Compd*. **293** (1999) 536.
7. W. Liu, H. Wu, Y. Lei, Q. Wang and J. Wu, *J. Alloys Compd*. **252** (1997) 234.
8. D.H. Ryan, F. Dumais, B. Patel, J. Kycia and J.O. Strom-Olsen, *J. Less-Common Metals* **172** (1991) 1296.
9. L. Sun, G.X. Wang, H.K. Liu, D.H. Bradhurst and S.X. Dou, *Electrochem. Solid-State Lett*. **3** (2000) 121.
10. B.D. Culity 'Elements of X-ray Diffraction', 2nd edn, (Addison-Wesley, Reading, MA, 1978) p. 101.
11. S.G. Zhang, Y. Haro, T. Morikawa, H. Inoue and C. Iwakura, *J. Alloys Compd*. **552** (1999) 293.
12. C. Iwakura, H. Inoue, S.G. Zhang and S. Nohara, *J. Alloys Compd*. **270** (1998) 142.
13. H. Inoue, H. Iden, R. Shin-ya, S. Nohara and C. Iwakura, *J. Electrochem. Soc*. **151** (2004) A939.
14. H.S. Chen, *Rep. Prog. Phys*. **43** (1980) 353.
15. P. Duwez, R.H. Willens and W. Klement Jr., *J. Appl. Phys*. **31** (1960) 1136.
16. T. Masumoto (Ed.), 'Materials Science of Amorphous Metals', (Ohm Pub., Tokyo, 1992).
17. S.S. Han, H.Y. Lee, N.H. Goo, W.T. Jeong and K.S. Lee, *J. Alloys Compd*. **330–332** (2002) 841.